

SAAPS

Satellite Anomaly Analysis and Prediction System

Technical Note 2

Satellite Anomaly Analysis Module

Version 0.2

ESA/ESTEC Contract No. 11974/96/NL/JG(SC)

P. Wintoft

3 April 2000

Document status sheet

Technical Note 2, SAAPS-SAAM	
Version	Date
0.1	16 December 1999
0.2	3 April 2000

Contents

1	Introduction	3
2	Satellite anomalies	4
2.1	Analysis of satellite anomalies	4
3	The satellite environment	6
3.1	LEO	6
3.2	GTO	6
3.3	GEO	6
3.4	The relation between geomagnetic activity and electron flux .	6
3.5	The relation between the solar wind and electron flux	6
4	The satellite anomaly analysis module	7
4.1	Basic operations	7
4.1.1	The output from the database	7
4.1.2	Handling data gaps	7
4.1.3	Averaging time series data	8
4.1.4	Error measures	9
4.2	Coordinate transformations	10
4.3	Entropy and mutual information	10
4.4	Linear correlation	11
4.5	Superposed epoch analysis	11
4.6	Pattern search	13
4.7	Determining the best prediction model	13
5	Various analyses	14
5.1	Entropies between different anomaly data sets	14
5.2	$\sum K_p$ and its relation to anomalies	15
5.2.1	Mutual information	15
5.3	Average MeV GOES electron flux and anomalies	17
5.4	Solar wind and anomalies	17

Chapter 1

Introduction

The satellite anomaly analysis module (SAAM) shall provide five different functions as described in the URD [*Wintoft, 1999*]: plotting functions, filters, statistics, guidelines, and estimate of the best prediction model. In this document it will be examined how this shall be achieved.

Chapter 2

Satellite anomalies

Problems are regularly experienced during the operation of satellites. These problems, or anomalies, range from change in the memory state in onboard computers to physical damage on circuitry. Lists of satellite anomalies exist in both public [Wilkinson, 1994] and non-public databases. The origin of the anomaly can either be the space environment or a technical problem. Several studies have shown clear links between the space environment and anomaly times [Wrenn and Smith, 1996] which makes it feasible to develop a system for the analysis and prediction of space environment induced anomalies.

2.1 Analysis of satellite anomalies

When a satellite is exposed to electrons with energies of 1-20 keV electric charge may build up on the surface of the satellite [Wrenn and Smith, 1996] and cause electrostatic discharge (ESD). Electrons in this energy range at GEO are accelerated by geomagnetic substorms and are thus clustered around the midnight-morning local time sector. The anomalies from the Marecs-A satellite show a clear clustering around 3 hours local time. The interpretation is thus that the anomalies are due to surface charging [Wrenn and Smith, 1996, Dyer and Rodgers, 1999]. [Wrenn and Smith, 1996] also studies the probability for Marecs-A anomalies as a function of both local time and Kp, where Kp serves as an indicator of keV electron flux. This type of analysis can be used to identify surface ESD effects.

Internal charging, or deep dielectric charging, can occur at times of enhanced fluxes of MeV electrons. Electrons are trapped in dielectric materials and charge can build up over several hours to a few days until a discharge may occur. [Wrenn and Smith, 1996] analyzed some 140 anomalies from the DRA δ satellite. A key feature of the anomalies were that they were preceded by a charging time of more than 30 hours. Based on this a correlation was made between the anomalies and the daily average flux of the > 2 MeV electrons measured at GOES-7. There was a clear threshold in the electron

flux below which no anomalies occurred.

[*López Honrubia and Hilgers, 1997*] studied five years of anomaly data from two consecutive Meteosat satellites, MOP-1 and MOP-2, together with the daily average electron flux for energies above 2 MeV. It was shown that there were a clear trend that the anomalies occur during days with high flux values. However, for individual anomaly events the flux values for the preceding days showed a large degree of variation with no unique pattern leading to the anomaly. Two different methods were applied to make a classification of the anomaly and non-anomaly events: a linear correlation method and a non-linear neural network.

Chapter 3

The satellite environment

3.1 LEO

3.2 GTO

3.3 GEO

3.4 The relation between geomagnetic activity and electron flux

3.5 The relation between the solar wind and electron flux

Chapter 4

The satellite anomaly analysis module

4.1 Basic operations

4.1.1 The output from the database

A time series of a parameter are obtained from the SAAPS database by calling the request method from the the database tool. All data, except the anomaly data, are contiguous. Any data gaps in the time series are indicated with NaN (Not a Number). The output from the database tool is a vector of objects, were each object contain the time of the observation and one or several data values depending on which parameter that has been requested. There are three arguments that must be specified when requesting data: the parameter, start time, and end time. E.g., if the requested parameter is the magnetic field data from the ACE spacecraft (ACE-MFI), for a period from t_0 to t_1 , then the database tool would return

$$X = \begin{bmatrix} t_0 & B(t_0) & B_x(t_0) & B_y(t_0) & B_z(t_0) \\ t_0 + \Delta t & B(t_0 + \Delta t) & B_x(t_0 + \Delta t) & B_y(t_0 + \Delta t) & B_z(t_0 + \Delta t) \\ \vdots & \vdots & \vdots & \vdots & \vdots \\ t_1 & B(t_1) & B_x(t_1) & B_y(t_1) & B_z(t_1) \end{bmatrix}, \quad (4.1)$$

where Δt is the sampling interval.

4.1.2 Handling data gaps

Generally, all the parameters in the SAAPS database contain occasional data gaps. To be able to make any further mathematical analysis these data gaps have to be treated.

The safest approach is to simply to create a data set in which the times with data gaps have been removed. However, this may lead to small data

sets.

The data gaps can also be replaced with linearly interpolated data values. This is achieved by searching one column at a time for NaN's and then interpolate the value. Data gaps can be contiguous and thus extend over several time steps. The number of time steps over which it is acceptable to interpolate must be given. This number can be estimated from e.g. a cross-correlation analysis. The algorithm for removing data gaps is given below.

1. Set i_1 to the first instance of NaN in $X(i, j)$ for column j .
2. If $X(i_1 + 1, j) = \text{NaN}$ set $i_2 = i_1 + 1$.
3. Continue with step 2 until $X(i_n + 1, j) \neq \text{NaN}$.
4. If $n \leq m$, where m is the maximum number of contiguous time steps to be interpolated, then

$$\hat{X}(i_k, j) = \frac{k}{n+1} (X(i_1 - 1, j) + X(i_n + 1, j)), 1 \leq k \leq n.$$

5. Set i_1 to the next instance of NaN after i_n .
6. Continue with step 2 for rows i and all columns j .

4.1.3 Averaging time series data

To be able to perform studies between parameters with different sample intervals an averaging must be performed to reduce the time resolution for the parameter with the highest sampling rate to the resolution of the parameter with the lowest sampling rate. Also, models may not require the highest sampling rate.

Assume that the original time series x_0, x_1, \dots, x_m are equidistant sampled at times $t_0^{(x)}, t_1^{(x)}, \dots, t_m^{(x)}$ where the sample interval is $\Delta t^{(x)}$. We thus have

$$x_i = x(t_i^{(x)}) = x(t_{i-1}^{(x)} + \Delta t^{(x)}). \quad (4.2)$$

We also assume that the resolution $\Delta T^{(x)}$ equals the sample interval, i.e. $\Delta T^{(x)} = \Delta t^{(x)}$. We now want to average and resample the time series x_i to a new time series y_j so that

$$y_j = y(t_j^{(y)}) = y(t_{j-1}^{(y)} + \Delta t^{(y)}), \quad (4.3)$$

where $t_j^{(y)}$ and $\Delta t^{(y)}$ are the new sample times and sample interval, respectively. The time resolution of the new series is $\Delta T^{(y)}$ and is not necessary

equal to the sample interval $\Delta t^{(y)}$. The relation between the two series becomes

$$y_j = \frac{1}{p} \sum_{i=sj}^{sj+p-1} x_i, \quad (4.4)$$

where the number of points to average is

$$p = \frac{\Delta T^{(y)}}{\Delta T^{(x)}} = \frac{\Delta T^{(y)}}{\Delta t^{(x)}} \quad (4.5)$$

and the point sample interval is

$$s = \frac{\Delta t^{(y)}}{\Delta t^{(x)}}. \quad (4.6)$$

The new sample times becomes

$$t_j^{(y)} = t_{sj}^{(x)} + \frac{\Delta T^{(y)} - \Delta t^{(x)}}{2} + t_{\text{off}}^{(y)}, \quad (4.7)$$

where we also introduce a time offset $t_{\text{off}}^{(y)}$. The time offset determines to which time an average belongs. E.g. if $t_{\text{off}}^{(y)} = 0$ then we have a central average. If $t_{\text{off}}^{(y)} = -(\Delta T^{(y)} - \Delta t^{(x)})/2$ then the time is in the beginning of the average interval (forward average), while if $t_{\text{off}}^{(y)} = (\Delta T^{(y)} - \Delta t^{(x)})/2$ it is at the end of the average interval (lagging average). From a physical point of view the central average is to prefer, while for real time operation the lagging average must be used. The hourly average data from the Space Environment Center (SEC) and the OMNI data set use forward average data.

The latest time in the original time series is $t_m^{(x)}$. When performing the average in Equation 4.4 the last position to use is $sj + p - 1$. This means that $sj + p - 1$ has a maximum value of m , thus $sj \leq m - p + 1$.

$\Delta T^{(y)}$ and $\Delta t^{(y)}$ should also be multiples of $\Delta t^{(x)}$ to ensure that p and s are integer numbers.

Any data gaps that exist in the time series that are averaged will also be present in the resulting time series. This means that if a times series with five minute resolution is averaged to one hour resolution, and if there is a NaN for one point, then that one hour interval will also be a NaN. If this is to be avoided the time series should first be interpolated to remove any NaN's.

4.1.4 Error measures

To asses the performance of a model several different error measures exist.

The mean-square-error (MSE) is defined as

$$\text{RMSE} = \frac{1}{n} \sum_{i=1}^n (x_i - y_i)^2. \quad (4.8)$$

The root-mean-square error (RMSE) is defined as

$$\text{RMSE} = \sqrt{\text{MSE}}. \quad (4.9)$$

The variance is closely related to the MSE and is defined as

$$\sigma^2 = \frac{1}{n-1} \sum_{i=1}^n (x_i - \bar{x})^2. \quad (4.10)$$

Taking the square root of the variance we get the standard deviation σ . The prediction efficiency (PE) [Detman, 1998] is the MSE normalized with respect to the variance

$$\text{PE} = 1 - \frac{\text{MSE}}{\sigma^2}. \quad (4.11)$$

If the MSE equals the variance the PE becomes 0, and if MSE is zero the PE becomes equal to 1. To compare different prediction techniques skill scores [Detman, 1998] can be used. The skill score (SS) is defined as

$$\text{SS} = 1 - \frac{\text{MSE}}{\text{MSE}_{\text{ref}}}, \quad (4.12)$$

where the MSE of the model is related to the MSE of a reference model (MSE_{ref}). If $\text{SS} > 0$ then the new model is better than the reference model, while if $\text{SS} < 0$ the new model is less good than the reference model.

4.2 Coordinate transformations

4.3 Entropy and mutual information

[Swingler, 1996] and [Deco and Obradovic 1996]

Assume that we have a discrete random variable X that can take m different discrete values x with probabilities $p(x)$. The entropy of X then becomes

$$H(X) = - \sum_x p(x) \ln p(x). \quad (4.13)$$

As $0 \leq p(x) \leq 1$ the entropy will always be positive. The entropy will be maximum for a uniformly distributed variable; $p(x) = 1/m$ gives $H(X) = \ln m$.

For two variables X_1 and X_2 we have the joint probabilities $p(x_1, x_2)$ and conditional probabilities $p(x_1|x_2)$ with the relation

$$p(x_1|x_2) = \frac{p(x_1, x_2)}{p(x_2)}. \quad (4.14)$$

Note that $p(x_1, x_2) = p(x_2, x_1)$ but $p(x_1|x_2) \neq p(x_2|x_1)$. Similarly we have the joint entropy

$$H(X_1, X_2) = - \sum_{x_1} \sum_{x_2} p(x_1, x_2) \ln p(x_1, x_2), \quad (4.15)$$

and the conditional entropy

$$H(X_1|X_2) = - \sum_{x_1} \sum_{x_2} p(x_1, x_2) \ln p(x_2|x_1). \quad (4.16)$$

Mutual information

$$I(X_1; X_2) = \sum_{x_1} \sum_{x_2} p(x_1, x_2) \ln \frac{p(x_1, x_2)}{p(x_1)p(x_2)}. \quad (4.17)$$

If the fraction $I(X_1; X_2)/H(X_2)$ is zero then it is not possible to predict X_2 from X_1 . If the fraction is one then there is a good chance that X_2 is predictable from X_1 .

Generalizable to higher dimensions X_1, X_2, \dots, X_n .

As an example we can study the mapping $y = \sin x$ on the interval $x \in [0, 2\pi]$. We bin the continuous values into discrete values with a bin size of 0.1 and calculate the probabilities $p(x)$, $p(y)$, and $p(x, y)$. The result is shown in Figure 4.1. The computed entropies are $H(X) = 3.45$ and $H(Y) = 2.35$ and the mutual information is $I(X; Y) = 1.88$. The fraction then becomes $I(X; Y)/H(Y) = 0.801$ and thus predicting y from x should be successful. On the other hand we have $I(X; Y)/H(X) = 0.546$ which means that making the inverse prediction $y \mapsto x$ is more difficult. By examining the sine curve or the probabilities we see that going from x to y is single valued while going from y to x is double valued.

4.4 Linear correlation

The linear correlation coefficient is calculated as

$$r = \frac{\sum_i (x_i - \bar{x})(y_i - \bar{y})}{\sqrt{\sum_i (x_i - \bar{x})^2} \sqrt{\sum_i (y_i - \bar{y})^2}}, \quad (4.18)$$

where \bar{x} is the mean of the x_i 's and \bar{y} is the mean of the y_i 's [Press et al., 1992].

4.5 Superposed epoch analysis

An efficient way to examine if there are trends in a parameter associated with a list of events is to use superposed epoch analysis. For this one needs a list of events and the size and location of the analysis window. Assume we have a list of anomalies at times

$$t_i, 1 \leq i \leq m. \quad (4.19)$$

Next, we set the analysis window to start at

$$t_i^{(s)} = t_i + p\Delta t, \quad (4.20)$$

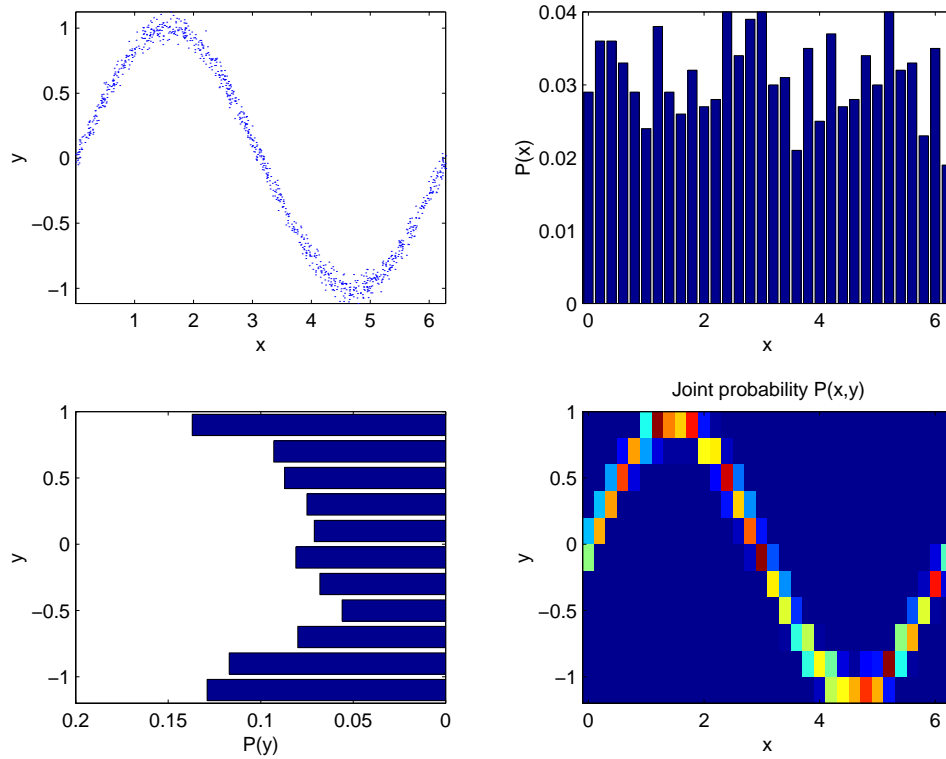


Figure 4.1: A sine curve $y = \sin x$ (top left) and the probabilities $p(x)$ (top right) and $p(y)$ (bottom left) using a bin size of 0.1, and the joint probabilities $p(x, y)$ (bottom right).

and end at

$$t_i^{(e)} = t_i + q\Delta t. \quad (4.21)$$

Generally $p < 0$ and $q \geq 0$ so that the window start before the event and end at or after the event. The sample interval for the parameter is Δt . A matrix is created from the parameter $x(t)$ that should be superposed as

$$X_{ij} = x(t_i^{(s)} + j\Delta t), \quad 0 \leq j \leq n, \quad (4.22)$$

where $n = q - p$. In the above it is assumed that the event times t_i are positioned at the sample times of the parameter $x(t)$. If this is not the case the event times are easily moved to the sample times by rounding the event time to the closest sample time. Then, the final step is to calculate the superposed values

$$s_j = \sum_{i=1}^m X_{ij}, \quad (4.23)$$

or alternatively the superposed average

$$\hat{s}_j = \frac{1}{m} s_j. \quad (4.24)$$

If there are any data gaps in the original time series $x(t)$ the matrix X_{ij} will contain NaN's at the corresponding positions. The value s_j at position j will then have a NaN if one or more rows of X_{ij} contain a NaN at position j . Obviously, if there are a large number of events (m large) then the probability that s_j will only contain NaN's increases. Therefore, it is desirable to replace data gaps with interpolated values.

4.6 Pattern search

4.7 Determining the best prediction model

Chapter 5

Various analyses

5.1 Entropies between different anomaly data sets

We can use the entropy measures introduced in Section 4.3 to examine the relation between the different anomaly data sets. To proceed with this we should as carefully as possible try to select the same type of anomalies for the sets that shall be compared. For the Marecs-A satellite we select all anomalies which are related to the A108 power voltage indicator, which are believed to be mainly related with surface ESD [*Wrenn and Smith, 1996*]. For the Meteosat-3 satellite we select all anomalies that are related to the radiometer and the Tele-X satellite the CMU reset related anomalies. Finally, we select the ESD anomalies from the NSSDC data set which include both surface and internal charging. The TDRS-1 set contains only SEU events.

Then we select two variables X and Y which corresponds to anomalies from two different satellites, respectively. X and Y can have the values $x = 0, 1$ and $y = 0, 1$, respectively, where a zero indicates no anomalies during a day and a one indicates one or more anomalies during the day. Table 5.1 summarises the joint probabilities, the total number of overlapping days, and the mutual information between any two sets. Each table cell contain the following:

$P(x = 0, y = 0)$ $P(x = 0, y = 1)$
 $P(x = 1, y = 0)$ $P(x = 1, y = 1)$
number of days $I(X; Y)/H(Y)$

If the fraction $I(X; Y)/H(Y)$ is zero the two variables are unrelated and if the fraction is one it is possible to predict Y from X .

As an example we can study the relation between the Marecs-A anomalies and the Meteosat-3 anomalies. In 73% of the days both satellites have no anomalies and in 4% of the days both satellites have anomalies. In 13% of the days Marecs-A have anomalies and at the same time Meteosat-3 have no anomalies. In 10% of the days Marecs-A show no anomalies while Meteosat-3 do. There is totally 2623 overlapping days between the two sets. Finally,

the relative mutual information is only 0.02. This means that there is a very weak relation between the Marecs-A A108 anomalies and the Meteosat-3 radiometer anomalies.

The strongest relation exist between the Tele-X and the NSSDC anomaly sets with $I(X; Y)/H(Y) = 0.11$. However, this is still very weak. It should also be noted that $P(x = 1, y = 1) = 0.01$ which means that there are only about 10 days out of the 1048 days when both satellites show simultaneous anomalies.

Table 5.1: Cross analysis between four different satellite anomaly sets. In each table cell is shown the joint probability $P(X, Y)$, the total number of days, and the mutual information divided by the entropy of Y ($I(X; Y)/H(Y)$). The satellite sets of the first columns corresponds to the variable X and the sets at the first row to the variable Y .

	Marecs-A		Meteosat-3		Tele-X		NSSDC	
Marecs-A	0.84	0.00	0.73	0.10	0.82	0.05	0.76	0.07
	0.00	0.16	0.13	0.04	0.11	0.02	0.13	0.04
	5143	1.00	2623	0.02	1729	0.03	4462	0.03
Meteosat-3	0.73	0.13	0.86	0.00	0.78	0.04	0.84	0.03
	0.10	0.04	0.00	0.14	0.15	0.03	0.12	0.01
	2623	0.02	2623	1.00	1601	0.04	2070	0.04
Tele-X	0.82	0.11	0.78	0.15	0.93	0.00	0.93	0.03
	0.05	0.02	0.04	0.03	0.00	0.07	0.03	0.01
	1729	0.02	1601	0.02	1973	1.00	1048	0.11
NSSDC	0.76	0.13	0.84	0.12	0.93	0.03	0.91	0.00
	0.07	0.04	0.03	0.01	0.03	0.01	0.00	0.09
	4462	0.02	2070	0.02	1048	0.10	7420	1.00

5.2 $\sum K_p$ and its relation to anomalies

5.2.1 Mutual information

We can examine the information content in $\sum K_p$ and relate it to the satellite anomalies. From past experience we know that the response of anomalies usually include the variation of $\sum K_p$ over several days. However, to calculate the mutual information we must bin $\sum K_p$ and assign one class to each bin. If we thus study a time delay line over 10 days we get (number of bins)¹⁰ combinations which becomes impossible to handle even if the number of bins is small. To be able to proceed we instead form averages of $\sum K_p$ extending from one to ten days. In this process some information is lost but we can get an overall picture of the situation.

We start with selecting all data in the five anomaly sets and compare it with the average $\sum K_p$. The result is shown in Figure 5.1. We see that

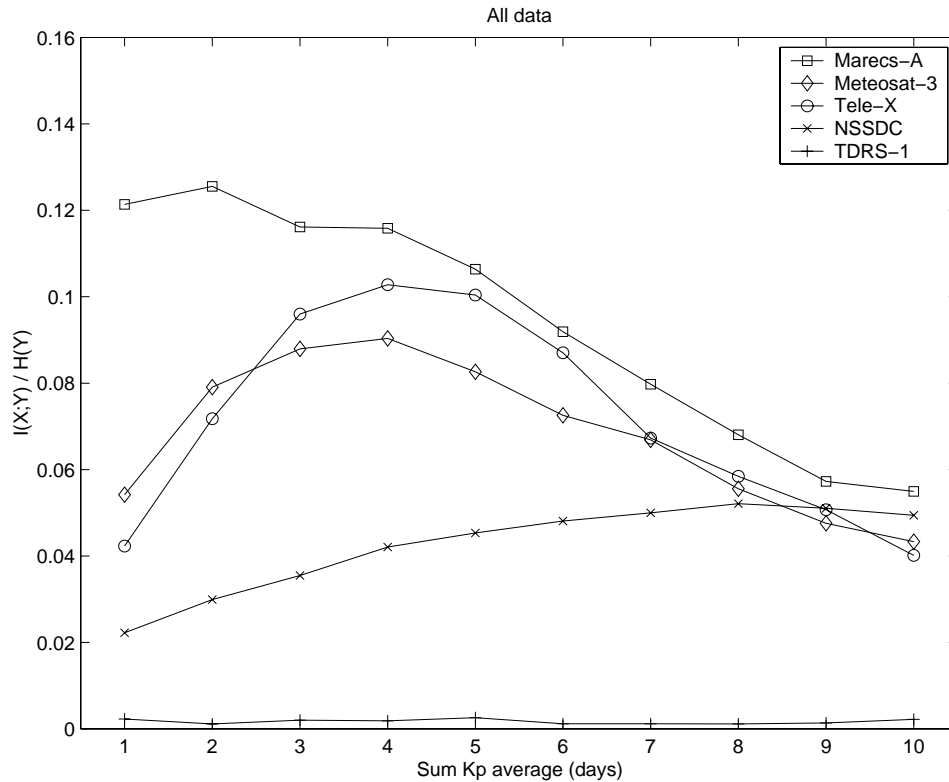


Figure 5.1: The relative mutual information $I(X;Y)/H(Y)$ for the different anomaly sets as a function of the average $\sum K_p$, where the average goes from 1 to 10 days. The anomaly sets contain all the anomaly data.

the relative mutual information (RMI) ($I(X;Y)/H(Y)$) is generally below 0.15 and that the different anomaly sets respond to $\sum K_p$ differently. The obvious fact is that the TDRS-1 have RMI ≈ 0 which is to expect as it contain only SEU anomalies. Marecs-A anomalies shows the most direct respons to $\sum K_p$ and Meteosat-3 and Tele-X anomalies are best related to about four days averages of $\sum K_p$.

We can refine the analysis by selecting a subset of the anomalies that are believed to be more related to $\sum K_p$. We make the same selection as in Section 5.1 which means that we have the surface ESD anomalies from Marecs-A, radiometer anomalies from Meteosat-3, CMU resets from Tele-X, and ESD anomalies from NSSDC. Now the relation between $\sum K_p$ and the anomalies becomes stronger as seen in Figure 5.2. The Marecs-A anomalies are best related to one to two day averages of $\sum K_p$, the Meteosat-3 anomalies for two to four day averages, Tele-X for three to five day averages, and NSSDC for seven to eight day averages. This is again a confirmation of the results shown in Table 5.1 that the anomalies are quite different for the

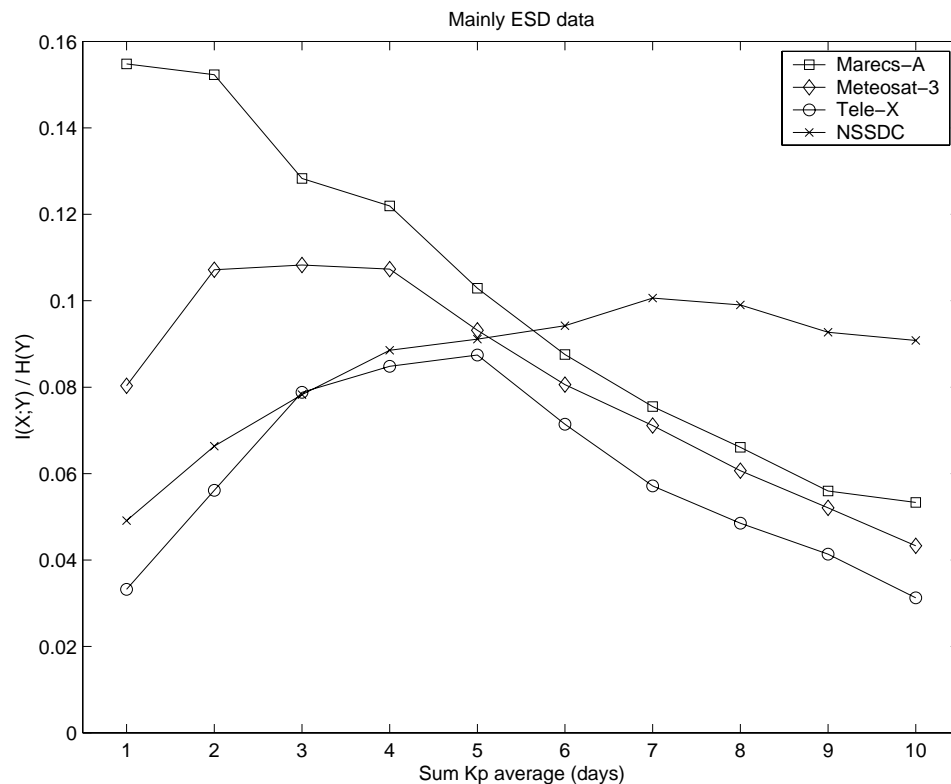


Figure 5.2: The relative mutual information $I(X;Y)/H(Y)$ for the different anomaly sets as a function of the average $\sum K_p$, where the average goes from 1 to 10 days. A subset of the anomaly data is selected that mainly related to ESD as explained in the text.

different satellites.

Finally, we can examine the effect of one day $\sum K_p$ delayed 0 to 9 days. The result is shown in Figure 5.3. We see that the Marecs-A anomalies are most related to $\sum K_p$ for the same day. The Meteosat-3 anomalies peaks at 1 day delay and Tele-X at 2 days.

5.3 Average MeV GOES electron flux and anomalies

5.4 Solar wind and anomalies

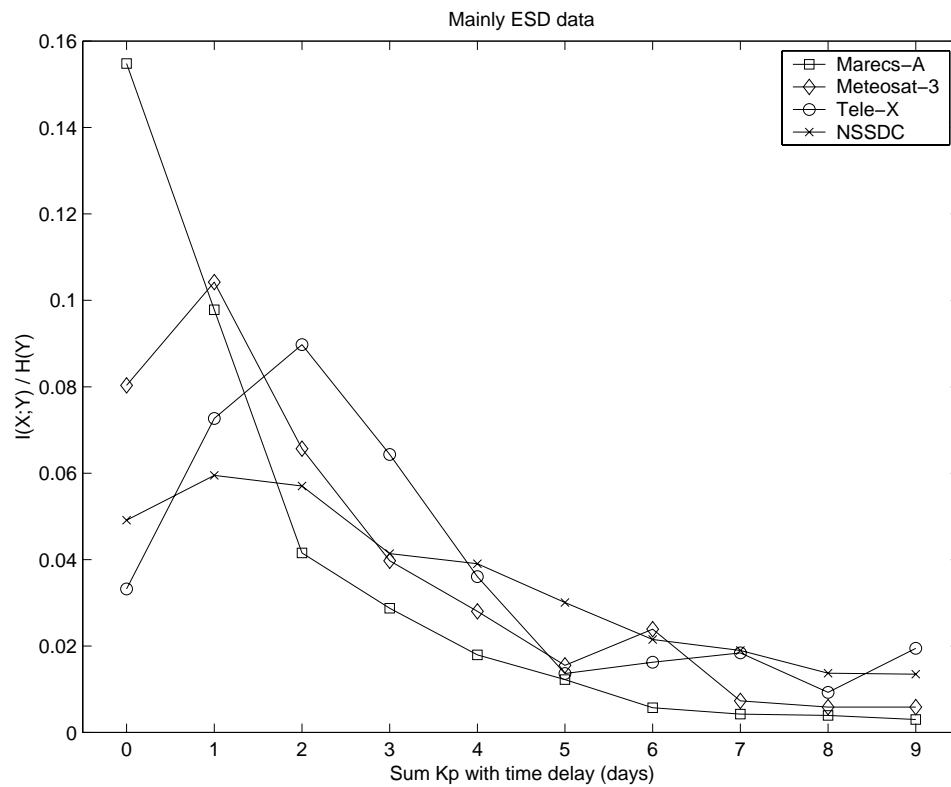


Figure 5.3: The relative mutual information $I(X;Y)/H(Y)$ for the different anomaly sets as a function of $\sum K_p$ delayed 0 to 9 days. A subset of the anomaly data is selected that mainly related to ESD as explained in the text.

References

- Deco, G., and D. Obradovic, *An Information-Theoretic Approach to Neural Computing*, Springer-Verlag, New York, 1996.
- Detman, T.R., Toward real-time operational model predictions, *Workshop on AI Applications in Solar-Terrestrial Physics*, Lund, Sweden, 29-31 July 1997, ESA, WPP-148, 135–143, 1998.
- Dyer, C., and D. Rodgers, Effects on spacecraft and aircraft electronics, *Workshop on space weather*, ESTEC, Noordwijk, WPP-155, 17–27, 1999.
- López Honrubia, F.J. and A. Hilgers, Some correlation techniques for environmentally induced anomalies analysis, *J. Spacecraft and Rockets*, 670–674, 1997.
- Press, W.H., S.A. Teukolsky, W.T. Vetterling, and B.P. Flannery, *Numerical Recipes in C*, Cambridge University Press, New York, 1992.
- Swingler, K., *Applying neural networks: a practical guide*, Academic Press Ltd, London, 1996.
- Wilkinson, D.C., Spacecraft Anomaly Manager, National Oceanic and Atmospheric Administration, National Geophysical Data Center, Solar-Terrestrial Physics Division, Boulder, CO, 1994.
- Wintoft, P., SAAPS WP 210 – Satellite Anomaly Analysis Module User Requirements Document, Version 1.1, 1999.
- Wintoft, P., SAAPS WP 120 – Technical Note 1, Satellite Anomaly Analysis Module, Version 0.1, 1999.
- Wrenn, G.L., and R.J.K. Smith, The ESD threat to GEO satellites: empirical models for observed effects due to both surface and internal charging, *ESA Symposium Proceedings on Environment Modelling for Space-based applications*, ESTEC, Noordwijk, SP-392, 121–124, 1996.
-